Relativistic calculations of coalescing binary neutron stars

JOSHUA FABER, PHILIPPE GRANDCLÉMENT and FREDERIC RASIO
Department of Physics and Astronomy, Northwestern University, Evanston,
IL 60208-0834, USA
E-mail: rasio@mac.com

Abstract. We have designed and tested a new relativistic Lagrangian hydrodynamics code, which treats gravity in the conformally flat approximation to general relativity. We have tested the resulting code extensively, finding that it performs well for calculations of equilibrium single-star models, collapsing relativistic dust clouds, and quasi-circular orbits of equilibrium solutions. By adding a radiation reaction treatment, we compute the full evolution of a coalescing binary neutron star system. We find that the amount of mass ejected from the system, much less than a per cent, is greatly reduced by the inclusion of relativistic gravitation. The gravity wave energy spectrum shows a clear divergence away from the Newtonian point-mass form, consistent with the form derived from relativistic quasi-equilibrium fluid sequences.

1. Introduction

It has long been recognized that coalescing binary neutron star (NS) systems are the first observable source of gravity waves (GW). With LIGO, GEO, and TAMA all taking scientific data, and VIRGO in the commissioning stage, it is increasingly important to have quantitatively accurate predictions of the GW signals we expect to measure during the merger process. Besides their use in aiding detection, these predictions are crucial for determining important physical information about the mass, radius, and equation of state (EOS) of NS from GW observations.

Calculations of binary NS coalescence have been performed for many years, beginning with studies in Newtonian gravity. It was recognized all along, however, that general relativity (GR) will play an important role during the merger, since the characteristic gravitational fields and velocities are squarely within the relativistic regime. As a result, increasingly sophisticated gravitational formalisms have been used in hydrodynamical calculations, starting with post-Newtonian treatments [1–5], many of which were based on a formalism developed by Blanchet *et al* [6] which includes all lowest-order 1PN effects as well as lowest order dissipative effects from gravitational radiation reaction losses. More recently, calculations have been

performed in full general relativity [7–9]. Unfortunately, the PN approximation breaks down during the merger when higher-order relativistic effects grow significant, and fully relativistic calculations typically introduce numerical instabilities which limit the amount of time for which a calculation will remain accurate. A middle ground is provided by the conformally flat (CF) approximation, developed originally by Wilson *et al* [10], which includes much of the non-linearity inherent to GR, but results in a set of coupled, non-linear, elliptic field equations, which can be evolved stably. We assume that the spatial part of the GR metric is equal to the flat-space form, multiplied by a conformal factor which varies with space and time, the metric taking the form

$$\mathrm{d}s^2 = -(N^2 - B_i B^i)\mathrm{d}t^2 - 2B_i\mathrm{d}t\mathrm{d}x^i + A^2\delta_{ij}\mathrm{d}x^i\mathrm{d}x^j. \tag{1}$$

While this approach cannot reproduce the exact GR solution for a general matter configuration, it is exact for spherically symmetric systems, and yields solutions which agree with those calculated using full GR to within a few per cent for many systems of interest [11].

2. Conformally flat SPH

After Shibata *et al* [12] calculated the evolution of coalescing NS binaries using a PN variant on the CF formalism, Oechslin *et al* [13] performed the first dynamical calculations which included all the non-linear effects present in the CF formalism. Unfortunately, the approach used in these efforts and many others throughout the history of this line of research is not particularly efficient. Solving the partial differential equations describing metric fields on large grids is very costly, both in terms of time and computer memory. Motivated by this conclusion, we combined our previous work in 3-d hydrodynamics with a spherical coordinates spectral methods code, which decomposes all field and hydrodynamical quantities into radial and angular functions. Our field solver, based on LORENE [14], is extremely efficient. The numerical libraries are publicly available at http://lorene.obspm.fr, and have been used previously, among other things, to construct the quasi-equilibrium binary configurations used in the aforementioned relativistic calculations. We combined this field solver with a smoothed particle hydrodynamics (SPH) evolution treatment, resulting in a 3-d code which can compute the full evolution of any number of relativistic matter configurations accurately and efficiently. Our code is, to the best of our knowledge, the first 3-d hydrodynamic evolution treatment of binary NS systems to use either spectral methods or spherical coordinates. For extremely detailed results, please refer to [15].

The field solver works by breaking up source terms into two distinct components, each centered on a star, which are further broken into radial domains, as shown in figure 1. In each domain, terms are evaluated at 'collocation points' spaced out in the radial and angular directions to handle any convex surface. Typically, solutions accurate to one part in 10^9 can be achieved quickly, using only a $17 \times 13 \times 12$ grid. The Lagrangian nature of SPH has several advantages over Eulerian grid-based methods for these calculations, first and foremost being the natural way it handles a surface; there are no particles where there is no matter.
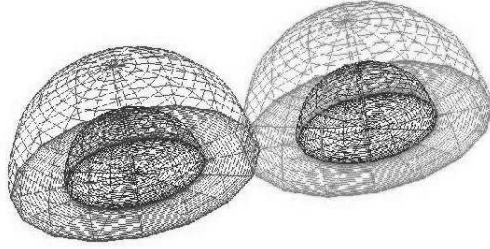
Figure 1. Radial domains used to solve the field equations of the CF method. Each vertex is a collocation point (from [14]).

3. Code tests

We have performed several tests to ensure that our code works properly. Since the CF formalism is known to be exact for spherically symmetric matter configurations, we calculated models of isolated neutron stars, finding excellent agreement with the well-known Oppenheimer–Volkov solution to well within a per cent for all hydrodynamic expressions and field values throughout the star.

To test the dynamical aspects of the code, we also computed the collapse of a dust cloud, i.e., pressureless matter, placed initially at rest. We compared our results to those of Petrich *et al* [16], who developed a semi-analytic procedure which yields the field values at all points in space-time, as well as the paths traced out by any given mass shell. We find that our code can reproduce the collapse extremely well, until just short of the point where the event horizon reaches the surface of the matter.

Since the CF formalism is time-symmetric, it does not contain terms which lead to gravitational radiation back reaction. Thus, we have tested our code by computing the evolution of quasi-equilibrium binaries, taken from the 'M14 vs. 14' sequence of [17]. We found that the binary separation and conserved system angular momentum vary by no more than 2.5% over two orbits, and the ADM mass is nearly constant for runs started at three different initial separations, including the innermost stable value found before a cusp forms. Similarly, a comparison of the field values and density profiles of the stars after two orbits yields very little deviation from the initial configuration. These results confirm for the first time that equilibrium binary configurations calculated by [17] are dynamically stable all the way to the appearance of a cusp.

4. Binary NS mergers

Dissipative effects can be added to the CF formalism through a radiation reaction potential which reproduces the lowest-order energy loss rate [10]. When radiation reaction is included, we find that the binary plunges rapidly toward merger soon after passing the point where a cusp is reached along the quasi-equilibrium sequence. In our approach, we have found that throughout the evolution, the NS surfaces can be modeled by triaxial ellipsoids that are allowed to rotate to match the growing
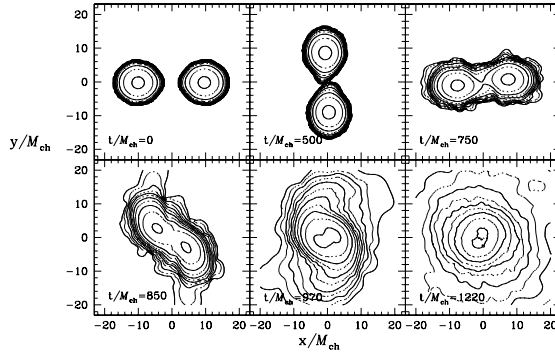
Figure 2. The evolution of the coalescing NS binary. Density contours are logarithmically spaced, two per decade. We see the development of significant tidal lag angles at $t/\mathcal{M}_{ch} = 500$, followed by an 'off-center' collision that leads to the formation of a vortex sheet and a small amount of matter ejection, finally resulting in a differentially rotating spheroidal configuration which is stable against gravitational collapse. Units are defined such that $G = c = 1$, and $\mathcal{M}_{ch}$ is the chirp mass of the system.

tidal lag angles. Field quantities are calculated by finding the SPH values for source terms at collocation points, and solving the field equations in the spectral basis. Field values are then interpolated back to SPH particles, with derivatives calculated to high accuracy by the field solver, rather than particle-based techniques. For overlapping configurations, we split our source terms between the two stars, weighting the density contributions such that each NS has a well-defined central density maximum, up until the point where the central density of the system allows us to treat the object as a single rapidly spinning body.

The evolution of the NS during a coalescence is shown in figure 2. In turn we see the inspiral of the NS, which orbit counterclockwise, with tidal lags growing as they do so. When the NS make contact, they collide in an 'off-axis' manner, with a very small amount of mass running along the surface interface before being spun off the newly forming remnant. This trace amount of matter, representing much less than 1% of the total system mass, remains gravitationally bound, forming a tenuous halo around the rapidly and differentially rotating 'hypermassive' remnant.

We calculate the GW signal produced during the merger in the lowest-order quadrupole limit, finding good agreement between our results and the relativistic calculations of [9]. In figure 3, we show the gravity wave signal in both polarizations, h_+ and $h_\times$, as functions of time. Prior to the merger, we see a 'chirp' signal, as the frequency and amplitude both increase while the stars approach each other. After a remnant forms, there is a period of modulated high-frequency emission, which damps away as the remnant relaxes toward a spheroidal shape.

While the time-dependence of the GW signal is important, it is perhaps more enlightening to look at the frequency dependence of the signal, and in particular, the energy spectrum dE_{GW}/df. Indeed, we have argued previously [18] that the changes in the total energy of quasi-equilibrium binary configurations for NS models with different compactness values M/R should leave an imprint on the energy

spectrum in the form of a 'break'. This can be observed by a narrow-band detector on an advanced interferometer such as LIGO II. Our argument is extremely straightforward: for a given sequence, we can calculate the total energy and GW frequency as a function of the binary separation, finding in general that the former is sensitive to the compactness of the NS, while the latter is not. After implicitly determining $E(f)$, we can numerically differentiate with respect to the GW frequency to find the energy spectrum. Relativistic effects typically flatten out the equilibrium energy curve with respect to the binary separation, which decreases the amplitude of the energy spectrum at the corresponding frequency. Using a parametrized model of these 'break frequencies', Hughes [19] determined that the NS radius could be determined to within a few per cent with at most $\sim$50 LIGO II observations of coalescing NS, and perhaps far fewer for optimal parameter values.

In order to avoid aliasing when taking the Fourier transform of the GW signal, we need to attach some estimate of the signal behavior both before and after the period which we calculate. Noting that the frequencies corresponding to remnant emission may be impossible to detect even with LIGO II, we fit the portion after our calculation with an exponentially damped oscillatory signal. The inspiral signal is much more important, but most groups have traditionally fit the inspiral by the lowest-order 'Newtonian' point-mass form [3,13]. This approach can lead to qualitatively inaccurate results, however, because it does not account for finite-size and relativistic corrections. Noting this, in FGR we calculated an inspiral wave-form directly from the quasi-equilibrium sequence which we used to construct our initial configuration. The inspiral wave form is thus completely consistent with our calculation.

Since our calculation was started from a quasi-circular orbit, we attach the inspiral wave-form onto our calculated merger wave-form at the point where the binary had attained the proper infall velocity, which we determined to be at $t = 250$. We note, however, that the exact point where the cross-over was made has virtually no effect on the resulting spectrum. In figure 4, we show as a solid line a complete and *consistent* relativistic wave-form for a binary NS merger. The frequencies listed on the upper axis assume typical parameters for NS: each has an ADM mass $M_0 = 1.4 M_\odot$. The two dotted lines show the com-
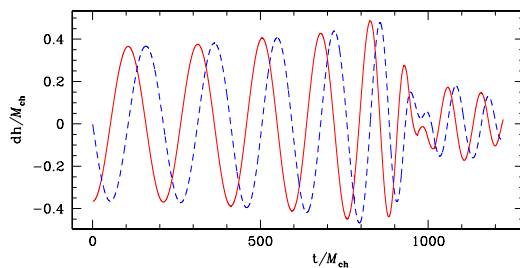

Figure 3. Gravitational wave signal in the h_+ (solid line) and $h_\times$ (dashed line) polarizations, for an observer located at a distance d from the system along the rotation axis. Units are as in figure 2. We see a chirp signal during the inspiral, followed by a lower-amplitude, modulated burst of high-frequency emission while the remnant forms.
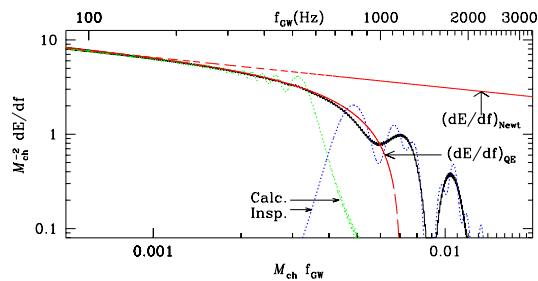
Figure 4. GW energy spectrum, $\mathcal{M}_{\mathrm{ch}}^{-2}\mathrm{d}E/\mathrm{d}f$, as a function of the GW frequency, $\mathcal{M}_{\mathrm{ch}}f_{\mathrm{GW}}$. The dotted lines show, respectively at high and low frequencies, the components contributed by our calculated signal and the quasi-equilibrium inspiral component. Also shown are the Newtonian point-mass energy spectrum (short-dashed line), and the quasi-equilibrium fit derived from equilibrium sequence data. On the upper axis, we show the corresponding frequencies in Hz assuming that each NS has an ADM mass $M_0 = 1.4M_\odot$. We see that the 'break frequency' occurs well within the sub-kHz regime.

ponents which make up the energy spectrum. At low frequencies, the primary contribution is from the inspiral wave-forms, and at high frequencies, from the calculated merger wave-form. The short-dashed line shows the Newtonian point-mass relation, $(\mathrm{d}E/\mathrm{d}f_{\mathrm{GW}})_{\mathrm{N}} = \pi^{2/3}\mathcal{M}_{\mathrm{ch}}^{5/3}f_{\mathrm{GW}}^{-1/3}/3$, and the long-dashed curve the fit we find from our quasi-equilibrium sequence data. We see excellent agreement between our calculated wave-form and the quasi-equilibrium fit, up until frequencies $\mathcal{M}_{\mathrm{ch}}f_{\mathrm{GW}} \approx 0.007$–$0.009$. This peak represents the 'piling up' of energy at the frequency corresponding to the phase of maximum GW luminosity, as the stars make contact and the infall rate drops dramatically. The second peak, at $\mathcal{M}_{\mathrm{ch}}f_{\mathrm{GW}} \approx 0.010$–$0.011$, represents emission from the ringdown of the merger remnant. It is likely that we underestimate the true height of this second peak somewhat, since we assume that the GW signal after our calculation damps away exponentially, but even for higher-amplitude peaks detections at these frequencies would be nearly impossible anyway.

In general, the energy spectrum we calculated confirms the general conclusions put forward in [3,18], albeit in a much more consistent way. The GW energy spectrum differs from the Newtonian point-mass form at frequencies much less than 1 kHz, within the range accessible to LIGO II. Thus, combining sub-kHz narrow-band detectors with broadband LIGO measurements, as suggested in [19], should allow GW measurements to constrain the NS compactness and EOS.

Acknowledgements

References

[1] J A Faber and F A Rasio, *Phys. Rev.* **D62**, 064012 (2000).
[2] J A Faber, F A Rasio and J B Manor, *Phys. Rev.* **D63**, 044012 (2001).
[3] J A Faber and F A Rasio, *Phys. Rev.* **D65**, 084042 (2002)
[4] S Ayal, T Piran, R Oechslin, M B Davies and S Rosswog, *Astrophys. J.* **550**, 846 (2001)
[5] M Shibata, K Oohara and T Nakamura, *Prog. Theor. Phys.* **98**, 1081 (1997)
[6] L Blanchet, T Damour and G Schaefer, *Mon. Not. R. Astron. Soc.* **242**, 289 (1990)
[7] M Shibata and K Uryu, *Phys. Rev.* **D61**, 064001 (2000)
[8] M Shibata and K Uryu, *Prog. Theor. Phys.* **107**, 265 (2002)
[9] M Shibata, K Taniguchi and K Uryu, *Phys. Rev.* **D68**, 084020 (2003)
[10] J R Wilson, G J Mathews and P Marronetti, *Phys. Rev.* **D54**, 1317 (1996)
[11] G J Mathews, P Marronetti and J R Wilson, *Phys. Rev.* **D58**, 043003 (1998)
[12] M Shibata, T W Baumgarte and S L Shapiro, *Phys. Rev.* **D58**, 023002 (1998)
[13] R Oechslin, S Rosswog and F Thielemann, *Phys. Rev.* **D65**, 103005 (2002)
[14] E Gourgoulhon, P Grandclément, K Taniguchi, J Marck and S Bonazzola, *Phys. Rev.* **D63**, 064029 (2001)
[15] J A Faber, P Grandclément and F A Rasio, gr-qc/0312097 (2003)
[16] L I Petrich, S L Shapiro and S A Teukolsky, *Phys. Rev.* **D31**, 2459 (1985)
[17] K Taniguchi and E Gourgoulhon, *Phys. Rev.* **D66**, 104019 (2002)
[18] J A Faber, P Grandclément, F A Rasio and K Taniguchi, *Phys. Rev. Lett.* **89**, 231102 (2002)
[19] S A Hughes, *Phys. Rev.* **D66**, 102001 (2002)